Solvent effects on two-line atomic fluorescence of indium

Qing N. Chan,[1,2,*] Paul R. Medwell,[1,3] Peter A. M. Kalt,[1,3] Zeyad T. Alwahabi,[1,2] Bassam B. Dally,[1,3] and Graham J. Nathan[1,3]

[1]Centre for Energy Technology, The University of Adelaide, Adelaide, South Australia 5005, Australia

[2]School of Chemical Engineering, The University of Adelaide, Adelaide, South Australia 5005, Australia

[3]School of Mechanical Engineering, The University of Adelaide, Adelaide, South Australia 5005, Australia

*Corresponding author: qing.chan@adelaide.edu.au

Received 19 August 2009; revised 18 January 2010; accepted 8 February 2010; posted 12 February 2010 (Doc. ID 115963); published 4 March 2010

We aim to investigate the potential of four different organic solvents, namely, acetone, ethanol, methanol, and isopropanol, and the organic-solvent–water mixtures as a seeding medium for the two-line atomic fluorescence technique. Water is used as the reference case. Indium, which has been previously shown to have suitable spectroscopic attributes, is chosen as the thermometry species in the present study. Acetone and methanol are shown to enhance the fluorescence signal intensity the most (approximately threefold to fivefold at stoichiometric conditions) when used. Acetone and methanol are shown to improve the fluorescence emission over the entire stoichiometric envelope of flame, most significantly in the rich combustion region, as well as a twofold enhancement in the signal-to-noise ratio.

OCIS codes: 120.1740, 120.6780, 300.2530.

1. Introduction

While many parameters are of fundamental importance to combustion systems, temperature remains one of the most dominant factors. The temperature of a flame characterizes the heat transfer process and controls many of the important chemical and physical processes. Information on the temperature field distribution in combustion systems provides important input for the improvement of theoretical models and the optimization of practical combustion devices. This information is required at a temporal resolution comparable with the time scales of the combustion processes under investigation. It is also desirable that the data be at least of a two-dimensional nature.

Laser diagnostics can provide *in situ* instantaneous, nonintrusive, and temporally and spatially precise quantitative temperature measurements unrivaled by alternative methods. A variety of laser-based thermometry techniques have been developed; however, most of these are limited to clean combustion environments and have not been optimized to operate in the presence of particles, such as dust, coal, or biomass, with soot being one of the most challenging. This limits the capacity to investigate and understand many systems of practical significance. Therefore, there is a need for development of laser-based thermometry techniques that are suitable for application in particle-laden environments.

One of the most experimentally simple, yet useful, laser thermometry techniques is Rayleigh scattering [1]. However, due to the elastic nature of the process, Rayleigh scattering is limited to very clean, particle-free situations. Filtered Rayleigh scattering has been developed to mitigate this interference, but remains impractical in highly particle-laden flows [2–4]. Raman-based thermometry has greater capacity to avoid interference from scattering, with coherent anti-Stokes Raman spectroscopy (CARS) being one of

0003-6935/10/081257-10$15.00/0

the most widely used [5]. CARS is more applicable to luminous and particle-laden flow than most other techniques. However, it has other limitations, such as experimental complexity, and a lack of spatial fidelity compared with other planar techniques [1,6].

Among the laser spectroscopic techniques employed in combustion science, laser-induced fluorescence (LIF) is probably the most widely applied [1]. LIF can be used for temperature measurements, offering stronger signals than those from Raman systems. The temperature is deduced from the species population according to Boltzmann distribution. LIF thermometry has most commonly been employed to probe *in situ* flame radical OH or seeded NO [7–9]. However, the narrow range of temperature and mixture fraction over which OH exists in a flame limits its general application for thermometry [10]. Likewise, NO-LIF has limitations because it can suffer from background interferences in the presence of soot [9].

A number of two-line techniques have been proposed and used for different diagnostic purposes. For aqueous systems, the use of two different laser dyes has been proposed [11]. For simultaneous thermometry and velocimetry, the use of liquid crystals has also been proposed [12]. Two-line phosphorescence using ZnO:Zn and ZnO:Ga has also been reported, with claims of short lifetimes enabling a reduction in background interference [13]. Visualization of the gas temperature distribution around flames with the use of two-color LIF has also been recently suggested [14]. However, the feasibility of these techniques in practical flame diagnostics is yet to be demonstrated.

Two-line atomic fluorescence (TLAF) is a two-line technique that offers promise to be a high-quality tool for temperature measurements in sooting and particle-laden flames [1,15]. TLAF is a laser-based thermometry technique that has many similarities to other LIF-based techniques, but utilizes a seeded atomic species. TLAF involves sequential shifted measurements of the Stokes and anti-Stokes direct-line fluorescence produced from the optical excitation of a three-level system. The flame temperature is subsequently deduced from the ratio of the two fluorescence signals. The frequency shift of the TLAF technique enables filtering to minimize interference from spurious scattering, allowing measurements to be performed in sooty environments. To provide good sensitivity over the temperature range encountered in flames, indium atoms are typically used as the seeded atomic species for TLAF [16–18]. With some notable exceptions [19], indium has previously been seeded into the flame as indium chloride dissolved in water.

Despite the potential of the TLAF technique, previous TLAF studies have been limited by poor signal-to-noise ratio (SNR), thus preventing single-shot measurements. The limitation of measuring mean temperature is acceptable in the context of laminar premixed flames; however, such average data are insufficient for study of more dynamic turbulent flames. With a view to improving the SNR and, hence, the accuracy of the TLAF measurements, the possibility of extending the technique into the nonlinear excitation regime has been examined by the authors [20]. The nonlinear regime TLAF (NTLAF) was shown to provide a superior signal relative to the conventional linear TLAF, leading to a significant reduction of single-shot uncertainty. The present work aims to further improve the signal quality of the NTLAF technique.

The use of organic solvents to enhance spectral line emission in flame photometry was first reported by Berry *et al.* [21] and has since been widely applied to various flame spectroscopic techniques involving the utilization of flames to convert dissolved samples into optically active entities. A number of previous studies have investigated the effects of the various physical and chemical parameters involved in the enhancement of the spectral line emission with the use of organic solvents in place of water as the seeding medium [22–25]. The physical effects influence the release rate of the solute into flame by factors such as the rate of evaporation of the droplets and the droplet size distribution. The chemical effects of the organic solvent influence the flame temperature and chemical kinetics directly through the combustion of the solvent in flame. The aim of these previous investigations has been to optimize the spectroscopic techniques by the combined physical and chemical effects of the organic solvents. These previous studies have focused on the improvement of the detection of the samples delivered to the flames, which are often only available in micro quantities.

The present study aims to investigate the potential to improve the signal quality of the NTLAF indium fluorescence images by the use of an organic solvent to replace water as seeding medium. It aims to exploit the physical effects of the organic solvent, with a secondary benefit of providing a small positive chemical influence of the solvent introduced on the properties (in particular the temperature) of the flame. These influences are explored for acetone, isopropanol, methanol, and ethanol, following earlier work to enhance emission in flame photometry [25]. In addition to the effect of the pure organic solvents, it aims to investigate the influence of mixtures of the organic solvent with water on the fluorescence signal. The study then aims to assess the influence of flame stoichiometry on fluorescence signal and on SNR for those organic solvents that are found to have performed most favorably. The fluorescence signal obtained with water as the solvent is used as the reference measurement. A laminar premixed flame is used to provide a uniform flame medium and to avoid the complexities associated with the use of turbulent and/or nonpremixed flames.

2. Methodology

A. Nonlinear Regime TLAF

For the present study, the species of interest is neutral atomic indium (the TLAF active species). Indium

is an attractive thermometry species because it has a good sensitivity over the 800 to 2800 K temperature range, covering most practical combustion scenarios [17]. In addition, both the excitation and detection wavelengths of indium are within the visible range (410.18 and 451.13 nm), where the interferences from the hydrocarbons and other natural combustion species are less pronounced [26].

The three energy levels of indium relevant to TLAF are shown in Fig. 1. The Stokes process requires 410.18 nm laser excitation ($5^2P_{1/2} \rightarrow 6^2S_{1/2}$ transition), and the subsequent fluorescence ($6^2S_{1/2} \rightarrow 5^2P_{3/2}$ transition) is detected at 451.13 nm. The anti-Stokes process uses 451.13 nm excitation ($5^2P_{3/2} \rightarrow 6^2S_{1/2}$ transition) and 410.18 nm detection ($6^2S_{1/2} \rightarrow 5^2P_{1/2}$ transition). A full description of the TLAF theory, especially incorporating the NTLAF, has been presented in a previous publication [20]. In brief, for the NTLAF method, it has been shown that the temperature may be determined as follows:

$$T = \frac{\Delta E_{10}/k}{\ln\left(F_{21} \times \left(1 + \frac{C_S}{I_{20}}\right)\right) - \ln\left(F_{20} \times \left(1 + \frac{C_A}{I_{21}}\right)\right) + C_T}. \quad (1)$$

Here, E_{10} is the energy difference between levels, F is the fluorescence intensity, and I is the incident laser energy. The other terms are constants. C_S and C_A are derived experimentally from the fluorescence versus irradiance plot for the two excitation schemes, while C_T is determined via calibration in a premixed flame. The subscripts refer to the transition between the energy levels (Fig. 1).

It has previously been shown that the calibration constants are independent of the fuel type and flame composition, within experimental uncertainty, for a range of premixed flames [20]. Given this independence from composition, it is anticipated that the technique will be applicable across the reaction zone of nonpremixed flames.

B. Transformation of Indium during its Passage Throughout the Flame

The process involved in the generation of neutral indium atoms from indium chloride solution are attributed to the following steps [22,23,27–29].

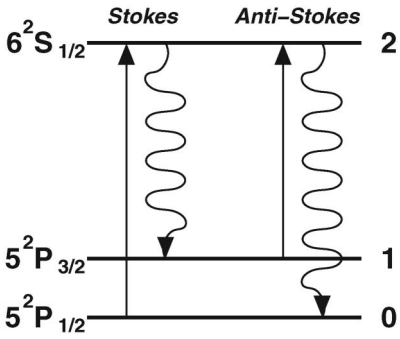

Fig. 1. Indium energy transitions employed in TLAF.

a. *Disintegration of the seeding solution*: an aerosol of droplets is formed from the nebulization of the seeding solution.

b. *Desolvation of the droplets*: the droplets are heated in the flame where the solvent is evaporated to form various metal complexes. Single ions and molecules are predominantly formed from the desolvation of the droplets with low solute concentration, while salt and ion clusters are predominantly formed from the desolvation of droplets with high solute concentration. Neutral or ionized molecules and fragments are subsequently released from the decomposition of the clusters.

c. *Gas phase ion/molecule and anion/cation recombination reactions*: the desolvated ions and molecules undergo different reactions, such as electron–ion recombination in the gas phase to form a variety of species with competing equilibria. These reactions are highly localized within the flame and are dependent on temperature and the chemical reactions within the region [30].

The species of interest, namely, neutral indium atom, is subsequently excited via laser irradiance with a species-specific wavelength.

Despite the complexity of the processes involved in the generation of neutral indium atoms in gas phase, the number of the thermally excited atoms within the probe volume can be well described by the Maxwell–Boltzmann distribution law [22,24]:

$$N^* \propto N \exp\left(-\frac{E}{kT}\right). \quad (2)$$

Here, the concentration of the neutral atoms in the excited state, N^*, is governed by the concentration of the neutral atoms in the ground state, N, and the temperature of the flame, T. The ground-state concentration of the neutral atoms within the probe volume is influenced by the effective supply of the solute to flame. The increase in the effective supply of the solute is brought about by factors such as improved nebulizer performance and increased solvent evaporation rate from the droplets. The change in temperature of the flame is directly influenced by the combustion of the seeding solution that is introduced with the solute [23,25].

C. Ultrasonic Nebulization

For the present study, an ultrasonic nebulizer is used to disintegrate the seeding solution into an aerosol of droplets. The electronically driven nebulizer utilizes ultrasonic vibrations, whose energy is derived from the piezoelectric transducer [31], to generate unstable surface waves at the liquid–air interface. The liquid sheet is fragmented and subsequently released into the surrounding air as very fine droplets [31–34]. This disintegration technique is characterized by fine droplets with a quite uniform size distribution. An empirical equation to estimate the droplet size from the ultrasonic nebulizer is described by Lang [32]:

$$D = 0.34\left(\frac{8\pi\sigma}{\rho F^2}\right)^{1/3}. \quad (3)$$

Here, D is the median diameter of the droplets, F is the exciting frequency of the ultrasonic nebulizer, σ is the surface tension, and ρ is the density of the liquid. Lang's correlation indicates no dependence of the droplet size on the liquid phase viscosity, which may be contrary to a number of experimental observations [31,35]. However, previous study has shown that Lang's correlation provides a reasonably accurate estimation when the effect of the liquid viscosity on the droplet size is negligible [33].

3. Experimental Setup

A. Experimental Overview

The details of the experimental layout, shown in Fig. 2, have been outlined in a previous publication [20]. In brief, two Nd:YAG pumped dye lasers are fired with 100 ns separation, to produce the required 410.18 and 451.13 nm excitation beams, with line widths of 0.4 and 0.3 cm^{-1}, respectively. The two beams are combined and circularly polarized with the use of a quarter-wave plate. The beams are subsequently directed through a cylindrical telescope lens system to produce a coplanar sheet of 4.5 mm thickness, 10 mm above the burner face. The spectral irradiance of each of the sheets is 0.25 $MW/cm^2/cm^{-1}$, which has previously been shown to be in the nonlinear excitation regime [20]. A thick light sheet is used in the current experiment to give improved SNR. The frequency-shifted fluorescence signals are subsequently detected through interference bandpass filters (FWHM = 10 nm, centered at 410 and 450 nm, respectively, 45% transmission) using two gated intensified CCD (ICCD) cameras with f-number 1.4 lenses, aligned nearly orthogonal to the laser sheet. The camera gate width of 50 ns is synchronized with the opposite wavelength excitation pulse to reject flame emission and elastic scattering. By appropriate image processing software, the resultant images from the cameras are spatially matched using a three-point matching algorithm and then morphed based on the cross correlation from a target image. These processing steps are implemented to ensure the corresponding images from the cameras are overlapped with subpixel accuracy.

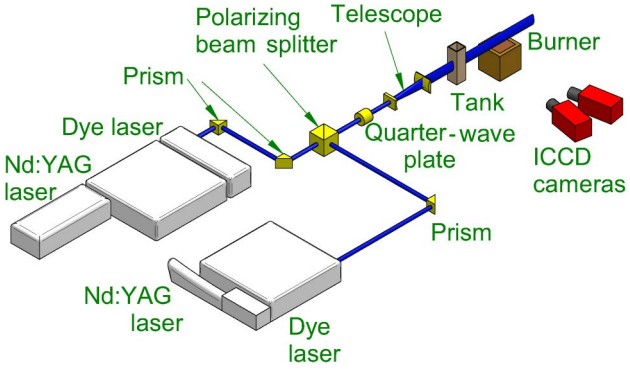

Fig. 2. (Color online) Schematic of experimental layout.

B. Burner and Seeding Arrangements

The laminar premixed flat-flame burner, shown in Fig. 3, was used. This burner provides a uniform, stable environment that enables comparisons to be made between different experimental cases. The burner face measures 50 mm × 50 mm and consists of a series of tubes fuelled with a premixture of natural gas and air. The air acts as a carrier gas to facilitate the seeding of indium. Much of the data presented in the first part of the study are collected when the flame stoichiometry (Φ) is unity. For the second part of the study, the stoichiometry of the flame was adjusted by varying the fuel flow rate at a constant oxidant flow rate to maintain a similar volumetric flow rate (and, thus, a similar seeded-indium concentration). The conditions of the natural gas/air flames used are shown in Table 1.

The seeder consists of an ultrasonic nebulizer that generates a mist of indium chloride dissolved in the seeding solution. A ballast volume is included between the seeder and the burner to damp any variations in the aerosol generation [36]. The ballast volume is also used to filter out larger droplets and to allow smaller droplets, which will undergo evaporation more readily, to be transported into the flame [23]. Four organic solvents are considered in this paper, namely, acetone, ethanol, isopropanol, and methanol, in addition to water. Selected physical properties at 20 °C and 1 atm of the solvents used in the present study are presented in Table 2. A concentration of 1.5 mg mL^{-1} is used for all seeding solutions to ensure linearity for the current seeding arrangement [20].

The temperature of the flames was measured with a fine-wire R-type thermocouple, with a bead diameter of 0.7 mm. The measured thermocouple readings were corrected for radiation losses by applying an energy balance to the thermocouple bead [37,38].

4. Results and Discussion

A. Effects of Solvents on Indium Fluorescence Emission

Figures 4(a) and 4(b) show typical instantaneous indium Stokes and anti-Stokes fluorescence images,

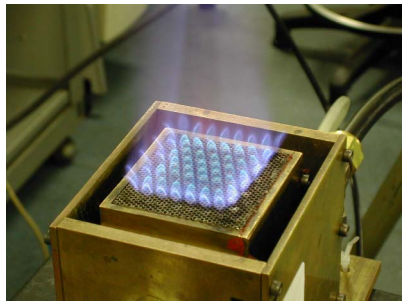

Fig. 3. (Color online) Photograph of the flat-flame burner and the premixed flame; here, firing natural gas. The burner matrix measures 50 mm × 50 mm.

Table 1. Premixed Flat-Flame Conditions

Mode	Fuel	Stoichiometry (Φ)	Bulk Velocity (m/s)	Temperature (K)
Premixed	Natural gas	0.91–1.80	0.27–0.29	1665–2165

Table 2. Selected Physical Properties of Solvents at 20 °C and 1 atm and Median Diameters of the Resultant Droplets Estimated Using Lang's Correlation

Solvent	Vapor Pressure (kPa)	Density (kg m^{-3})	Viscosity (cP)	Surface Tension (mN m^{-1})	Polarity index	Diameter (μm)
Acetone	24	790	0.32	25	5.1	2.21
Ethanol	5.9	789	1.18	22	4.3	2.12
Isopropanol	4.4	786	2.27	21	3.9	2.09
Methanol	12.3	792	0.58	23	5.1	2.15
Water	2.3	1000	1.00	73	10.2	2.92

respectively, from the laminar premixed natural gas flat flame, collected simultaneously under a laser spectral irradiance of 0.25 $MW/cm^2/cm^{-1}$. Each image has been spatially matched and corrected for background and detector attenuation. The images are ~20 mm high and 50 mm wide, centered at a 20 mm height above burner (HAB). All data is extracted from the central region, as indicated by the dashed area in Fig. 4, where the indium fluorescence is most uniform.

1. *Fluorescence—Solvents*

To assess the physical effects of the solvents on the spectral line emission, Fig. 5 presents the data obtained from a 150-shot average of both the Stokes and anti-Stokes fluorescence for the solvents selected. As a reference, the fluorescence signals are normalized with respect to the fluorescence signal recorded when water is used. The concentration of the indium salt was maintained at 1.5 mg mL^{-1} for all the seeding solutions used. This ensures that any change in the indium fluorescence observed is solely a function of the solvent used, rather than an effect of differing indium salt concentration within the solvents. Additionally, the flame stoichiometry was maintained at unity during the course of the experiment. This makes certain that any change in the fluorescence signal can be attributed entirely to the physical effects, i.e., negligible chemical influence on the properties of the flame. Thermocouple measurements show that the flame temperature varies by less than 40 K with the different solvents, eliminating any influence of this parameter on the fluorescence emission.

From Fig. 5, it is apparent that there is a threefold to fivefold gain in fluorescence signal, when organic solvents (excluding isopropanol) are used instead of water. Acetone and methanol, in particular, are observed to have intensified the fluorescence emission the most. The increase in the emission when organic solvents are used can be explained by the dependence

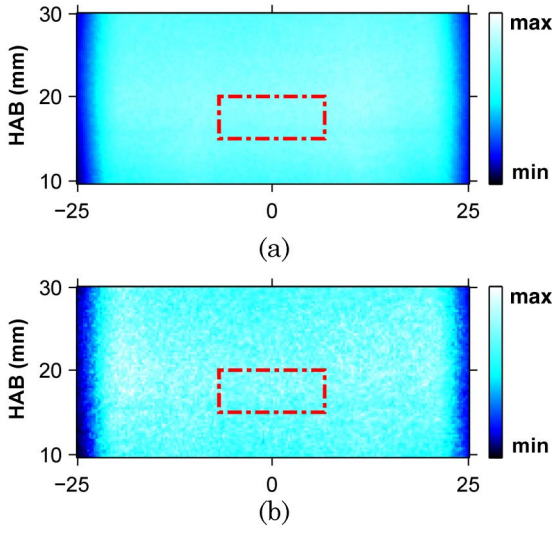

Fig. 4. (Color online) Typical instantaneous images of (a) Stokes and (b) anti-Stokes fluorescence in a laminar premixed natural gas flat flame. Dashed area indicates data extraction area. Laser propagates from left to right. HAB, height above burner.

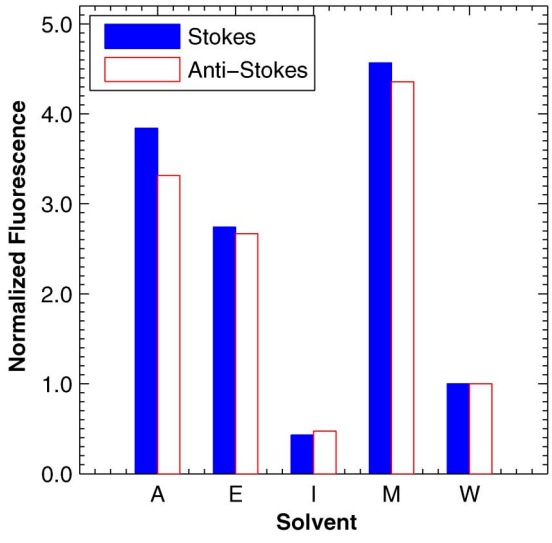

Fig. 5. (Color online) Normalized indium Stokes and anti-Stokes fluorescence for five different seeding solutions: A, acetone; E, ethanol; I, isopropanol; M, methanol, and W, water, for a flame stoichiometry of 1.0.

of the nebulizer performance on the viscosity and the surface tension of the solutions [39]. Organic solvents, such as acetone, ethanol, and methanol, have lower viscosity and surface tension values than water (Table 2). This eases the disintegration process, allowing droplets with smaller sizes (Table 2) to be generated at a more rapid rate. The droplet sizes are estimated using Lang's correlation (Eq. (3)). Sindayihebura *et al.* [33] have shown that the effect of liquid viscosity on the diameters of the droplets is negligible for the methanol–water and glycerol–water mixtures used in their investigation. This, combined with the knowledge that the estimated values are well within the range of droplet sizes (1–5 μm) typically generated from ultrasonic nebulization [31], justifies the use of the Lang correlation for the present study. Additionally, these organic solvents have a higher vapor pressure than water (Table 2), making the resultant droplets more evaporative and hence leading to a reduction in the amount of droplets persisting into the flame [22]. Together, these factors enhance the disintegration and desolvation process and, hence, the effective supply of the solute, namely indium chloride, into the flame. The increase in the effective supply of the solute leads to an increase in the concentration of indium species in flame. This explains the stronger fluorescence emission observed.

It is also interesting to note that, even though isopropanol has more favorable physical properties (lower surface tension and higher vapor pressure) than water (Table 2), Fig. 5 shows a drop in the fluorescence emission when isopropanol is used in place of water. The drop in the emission can be explained by the low solubility of the polar indium salt in isopropanol. The nonpolarity of isopropanol, as indicated by the low polarity index [40] in Table 2, is responsible for this low solubility and leads to a reduction in the transportation of the solute into the flame and hence also the fluorescence emission. This finding indicates that there are limits to the types of organic solvent that can be used to enhance the fluorescence emission from the flame due to the polar nature of the indium chloride salt.

2. *Fluorescence—Organic-Solvent–Water Mixtures*

The TLAF process is affected by a combination of processes (Section 2) that produce the TLAF active species. Most of these processes utilize little heat as compared with the heat released in a combustion reaction [19,23]. An exception to these processes is desolvation, which can consume a significant fraction of the heat content, leading to a 100–150 K cooling of the flame [15,20]. This reduction in the flame temperature is significant and will change the combustion processes, so should be avoided if possible.

The indium Stokes and anti-Stokes fluorescence are plotted as a function of the volume fraction for the organic solvents within the seeding solution. This is to investigate the feasibility of using an organic-solvent–water mixture whose enthalpy of reaction matches the latent heat of vaporization and also provides a reasonable gain in fluorescence signal. To assess this, the volume fraction of the organic solvent and distilled water within the seeding solution were varied. Again, the concentration of the indium salt within the seeding solution was maintained at 1.5 mg mL^{-1}.

Figure 6 presents the data obtained from a 150-shot average of both the Stokes and the anti-Stokes fluorescence for four organic-solvent–water mixtures. Figure 6 shows that, for the present burner system arrangement, the fluorescence signals for acetone, ethanol, and methanol (normalized by the fluorescence signal recorded with water) increase with the concentration of the organic solvents within the seeding solution. However, the dependence is not linear. Rather, a sudden increase in the emission occurs when the volume fraction of the organic solvents within the seeding solution exceeds ~0.8. This observation implies that, even though enhancement is

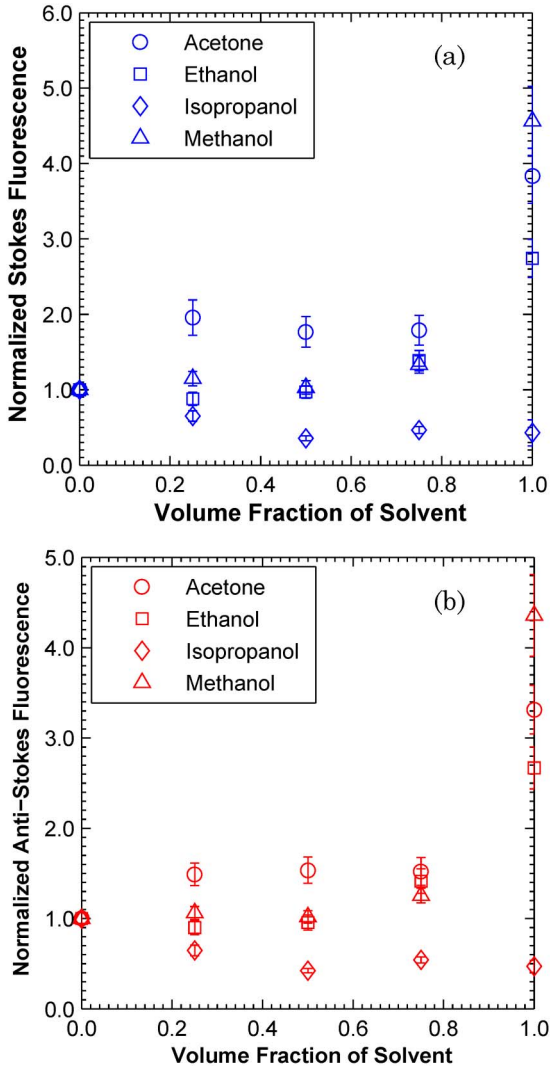

Fig. 6. (Color online) Normalized indium (a) Stokes and (b) anti-Stokes fluorescence over a range of concentration of organic solvents within seeding solution, balanced with distilled water.

attainable with the use of organic-solvent–water mixtures; almost pure organic solvents are needed to achieve significant intensification. A volume fraction of ~0.1 (significantly less than the amount required for sufficient intensification) corresponds to the concentration of each of the organic-solvent–water mixtures needed to match the enthalpy of the reaction with the latent heat of vaporization of the mixture within flame. Hence, no benefit in using organic-solvent–water mixture was found. Rather, these findings suggest that pure organic solvents should be used. The use of isopropanol as the solvent was found to reduce the fluorescence, consistent with the finding reported above.

Stokes fluorescence has been shown to have a higher SNR than anti-Stokes [20]. Since the temperature is determined from the ratio of the two signals, the latter controls the SNR. Additionally, both Stokes and anti-Stokes are observed to display similar characteristics throughout the present study. Hence, only the anti-Stokes fluorescence results are presented and discussed in the subsequent sections.

B. Effects of Selected Organic Solvents on Indium Fluorescence across the Flame Stoichiometric Envelope

1. *Fluorescence—Stoichiometry*

Comparison between the effectiveness of acetone and methanol, which are shown in Subsection 4.A.1 to have performed most favorably, is made across the stoichiometric envelope of the premixed flame. Figure 7 presents the measured anti-Stokes fluorescence emission from these flames, with acetone, methanol, or water (reference case) used as the seeding solution. Error bars (1 standard deviation) are used in the figure to show the variability in the measurements.

It is readily apparent from Fig. 7 that the fluorescence increases as the stoichiometry of the flame increases, over the range of $0.9 < \Phi < 1.4$. This indicates that the neutral indium atoms are produced more effectively when the flame is rich [15,19,41]. The process by which the indium is converted into free atoms is dependent on numerous factors, such as the temperature and the chemical conditions. The lower fluorescence signal emission in the lean combustion region is caused by the less suitable chemical condition due to the abundance of oxidizing species. Beyond a stoichiometry of unity, the fluorescence signal is observed to continue increasing, despite a reduction in flame temperature. This highlights the importance of the local chemical environment on the indium fluorescence signal. The chemical conditions beyond $\Phi = 1.4$ are apparently insufficient to counteract the further reduction in temperature beyond this stoichiometry.

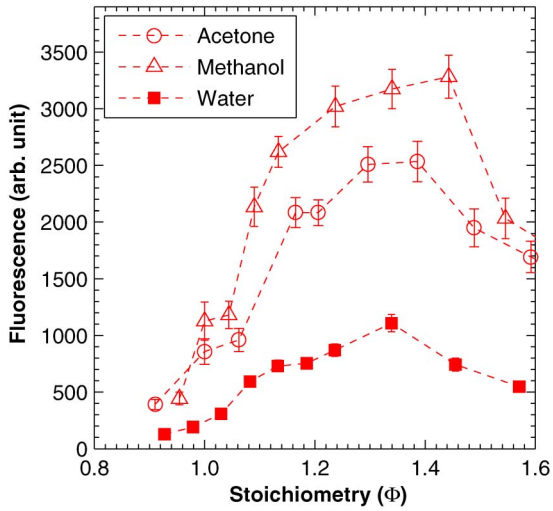

Fig. 7. (Color online) Indium anti-Stokes fluorescence as a function of flame stoichiometry.

Figure 7 demonstrates a substantial increase in the fluorescence intensity across the stoichiometric envelope of the flame when the organic solvents are employed. The enhancement is threefold to fivefold across the stoichiometric envelope when acetone or methanol is used, and is higher with methanol. This suggests that the release rate of the solute improves the most with methanol.

The higher gain in the fluorescence emission appears to be explained by the finer methanol droplets relative to acetone and water (Table 2). The surface area per unit volume is inversely proportional to the droplet size. Methanol, which has the smallest droplet size, has the largest surface area per unit volume. The methanol droplets are desolvated at a faster rate than acetone and water droplets, resulting in the highest rate of release of solute and, hence, fluorescence emission, as observed. It is interesting to note that the measured nebulization rate of acetone is ~1.5 times (volumetric) higher than that of methanol. Furthermore, acetone vaporizes easier than methanol, as indicated by the higher vapor pressure in Table 2. Together, these findings show that, despite the higher nebulization rate and volatility of the droplets when acetone is used, the effective supply of solute to flame is enhanced the most when methanol is used as seeding solution.

2. *Normalized Fluorescence—Stoichiometry*

The anti-Stokes fluorescence signals, normalized by the local maximum fluorescence values, are shown in Fig. 8. The normalized curves are observed to display similar characteristics over the range of flame stoichiometries presented. The good overlapping of the profiles, despite the differences in the properties of the solvents, suggests that any chemical influence of the organic solvents is small. Rather, the influence on fluorescence signal is dominated by the capacity to supply solute to the flame. The overlap of the profiles also indicates that the profiles are proportional with a factor that is constant over the tested range of flame stoichiometries. This finding further validates the comparisons of the various solvents and solvent–water mixtures at a single flame condition in

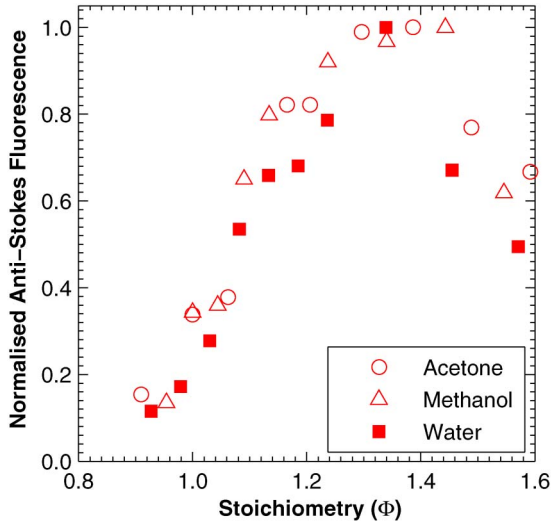

Fig. 8. (Color online) Normalized anti-Stokes fluorescence signal as a function of flame stoichiometry.

Subsections 4.A.1 and 4.A.2, because the differences between the solvents are observed to be consistent for all flame stoichiometries.

3. *Relative Gain in Signal-to-Noise Ratio—Stoichiometry*

To further assess the effectiveness of the organic solvents in enhancing the fluorescence signal, the relative gain in the SNR over the stoichiometric envelope of the flame is presented in Fig. 9. Error bars (1 standard deviation) are used in the figure to show the variability in the measurements. SNR is defined here as the ratio of the average signal intensity to the interpixel noise. This figure was obtained by comparing the SNR of the anti-Stokes fluorescence images obtained with acetone and methanol with water over a range of flame stoichiometries. Figure 9 shows that

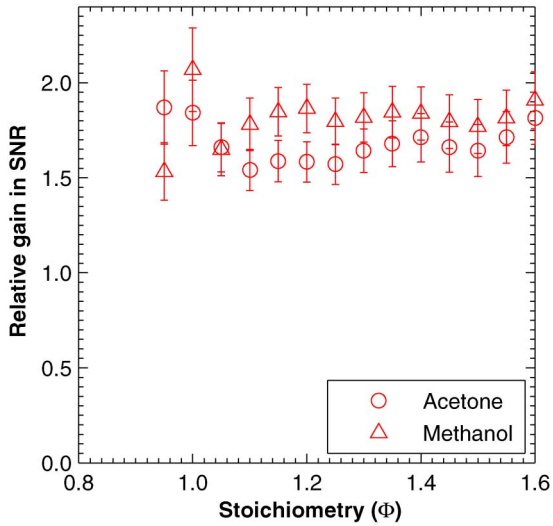

Fig. 9. (Color online) Relative gain in SNR of the indium anti-Stokes fluorescence, as compared to water, as a function of flame stoichiometry.

methanol and acetone enhance the SNR of the fluorescence image across the stoichiometric envelope of the flame. The gain in SNR is observed to be relatively invariant at ~1.8 above a flame stoichiometry of ~1.1. The observed invariant profile appears to be explained by the more efficient neutral indium atom formation process in the fuel-rich region, counteracting the drop in fluorescence signals due to the drop in flame temperature (in accordance with Eq. (2)) in the richer region. Some scatter in the data, coupled with larger error bars, is observable in the lean region of the flame. This is to be expected due to the lack of active indium species in such an environment.

4. *Signal-to-Noise Ratio of Temperature Images—Solvents*

Figure 10 presents histograms obtained from an instantaneous temperature image of the premixed

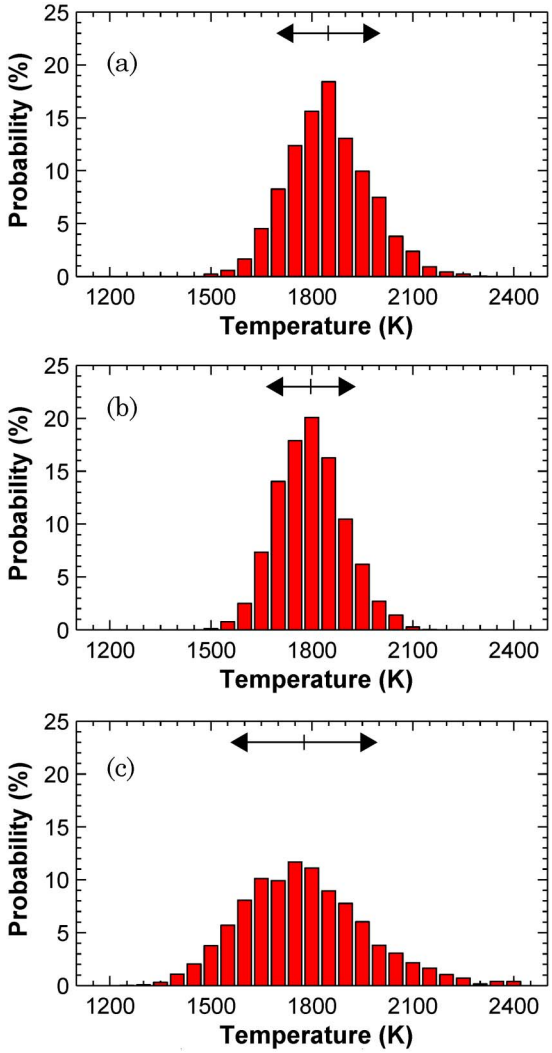

Fig. 10. (Color online) Temperature histograms from single instantaneous images of laminar premixed flame with a flame stoichiometry of ~1.55 with (a) acetone, (b) methanol, and (c) water as seeding solution. Double-headed arrows indicate the temperature spans that are associated with 1 standard deviation.

laminar flames collected with acetone, methanol, and water as seeding solutions, at a flame stoichiometry of ~1.55. The histograms demonstrate that the use of the organic solvents provides a significant improvement in SNR, as indicated by reduced temperature span, and the increased probability at the expected temperature (~1800 K) of the flame. Double-headed arrows are also used to indicate the temperature spans that are associated with 1 standard deviation from the mean. Hence, a reduction in the single-shot uncertainty of the temperature images results.

5. Conclusion

This paper has compared the potential use of four different solvents, namely acetone, ethanol, isopropanol, and methanol, to replace water as the seeding medium for TLAF. The benefit of the organic solvents is attributed mainly to combined influence of the more favorable physical properties that control the rate at which indium species is seeded into the flame, such as surface tension, solubility, and vapor pressure. Acetone and methanol have been shown to yield the highest gain in the fluorescence signal intensity (approximately threefold to fivefold). No significant benefit is observed with the use of organic-solvent–water mixtures. Acetone and methanol have been shown to enhance the SNR of the fluorescence emission throughout the stoichiometric envelope of the flame, with the most significant enhancement (approximately twofold) observed in the rich combustion region. Acetone and methanol have also been demonstrated not to have a detrimental effect on the neutral indium formation process. The identification of the potential of the organic solvents, specifically acetone and methanol, in enhancing the fluorescence signal represents a significant development to support future imaging applications in turbulent or/and sooting flames where the background interferences are expected to be more pronounced.

The authors would like to thank the Centre for Energy Technology (CET) at The University of Adelaide for their support. The Australia Research Council (ARC) is also gratefully acknowledged for their support of this work through ARC Discovery and Linkage Infrastructure, Equipment and Facilities (LIEF) grant schemes. The authors are also grateful to Gregory Metha for his invaluable input in the planning of this work.

References

1. K. Kohse-Höinghaus and J. B. Jeffries, *Applied Combustion Diagnostics* (Taylor and Francis, 2002).
2. D. Hoffman, K. U. Münch, and A. Leipertz, "Two-dimensional temperature determination in sooting flames by filtered Rayleigh scattering," Opt. Lett. **21**, 525–527 (1996).
3. D. Hofmann and A. Leipertz, "Temperature field measurements in a sooting flame by filtered Rayleigh scattering (FRS)," Proc. Combust. Inst. **26**, 945–950 (1996).
4. S. P. Kearney, R. W. Schefer, S. J. Beresh, and T. W. Grasser, "Temperature imaging in nonpremixed flames by joint filtered Rayleigh and Raman scattering," Appl. Opt. **44**, 1548–1558 (2005).
5. M. Afzelius, P. E. Bengtsson, J. Bood, C. Brackmann, and A. Kurtz, "Development of multipoint vibrational coherent anti-Stokes Raman spectroscopy for flame applications," Appl. Opt. **45**, 1177–1186 (2006).
6. A. Burkert, W. Triebel, H. Stafast, and J. König, "Single-shot imaging of gas temperatures in low-temperature combustion based on laser-induced fluorescence of formaldehyde," Proc. Combust. Inst. **29**, 2645–2651 (2002).
7. A. T. Hartlieb, B. Atakan, and K. Kohse-Höinghaus, "Temperature measurement in fuel-rich non-sooting low-pressure hydrocarbon flames," Appl. Phys. B **70**, 435–445 (2000).
8. R. Cattolica, "OH rotational temperature from two-line laser excited fluorescence," Appl. Opt. **20**, 1156–1166 (1981).
9. J. M. Seitzman, R. K. Hanson, P. A. DeBarber, and C. F. Hess, "Application of quantitative two-line OH planar laser-induced fluorescence for temporally resolved planar thermometry in reacting flows," Appl. Opt. **33**, 4000–4012 (1994).
10. J. Nygren, J. Engström, J. Walewski, C. F. Kaminski, and M. Aldén, "Applications and evaluation of two-line atomic LIF thermometry in sooting combustion environments," Meas. Sci. Technol. **12**, 1294–1303 (2001).
11. G. A. Robinson, R. P. Lucht, and N. M. Laurendeau, "Two-color planar laser-induced fluorescence thermometry in aqueous solutions," Appl. Opt. **47**, 2852–2858 (2008).
12. D. Dabiri, "Digital particle image thermometry/velocimetry: a review," Exp. Fluids **46**, 191–241 (2009).
13. G. Särner, M. Richter, and M. Aldén, "Two-dimensional thermometry using temperature-induced line shifts of ZnO:Zn and ZnO:Ga fluorescence," Opt. Lett. **33**, 1327–1329 (2008).
14. T. Hirasawa, Y. Kamata, T. Kaneba, and Y. Nakamura, "Visualization of ambient gas temperature based on two-color LIF," in *9th Asia–Pacific Conference on Combustion* (National Taiwan University, 2009), paper 10092.
15. J. Engström, J. Nygren, M. Aldén, and C. F. Kaminski, "Two-line atomic fluorescence as a temperature probe for highly sooting flames," Opt. Lett. **25**, 1469–1471 (2000).
16. M. Aldén, P. Grafström, H. Lundberg, and S. Svanberg, "Spatially resolved temperature measurements in a flame using laser-excited two-line atomic fluorescence and diode-array detection," Opt. Lett. **8**, 241–243 (1983).
17. H. Haraguchi, B. Smith, S. Weeks, D. J. Johnson, and J. D. Winefordner, "Measurement of small volume flame temperatures by the two-line atomic fluorescence method," Appl. Spectrosc. **31**, 156–163 (1977).
18. I. S. Burns, J. Hult, and C. F. Kaminski, "Spectroscopic use of a novel blue diode laser in a wavelength region around 450 nm," Appl. Phys. B **79**, 491–495 (2004).
19. C. F. Kaminski, J. Engström, and M. Aldén, "Quasi-instantaneous two-dimensional temperature measurements in a spark ignition engine using 2-line atomic fluorescence," Proc. Combust. Inst. **27**, 85–93 (1998).
20. P. R. Medwell, Q. N. Chan, P. A. M. Kalt, Z. T. Alwahabi, B. B. Dally, and G. J. Nathan, "Development of temperature imaging using two-line atomic fluorescence," Appl. Opt. **48**, 1237–1248 (2009).
21. J. W. Berry, D. G. Chappell, and R. B. Barnes, "Improved method of flame photometry," Ind. Eng. Chem. Anal. Ed. **18**, 19–24 (1946).
22. J. H. Gibson, W. E. L. Grossman, and W. D. Cooke, "Excitation process in flame spectroscopy," Anal. Chem. **35**, 266–277 (1963).
23. J. A. Dean and C. T. Rains, *Flame Emission and Atomic Absorption Spectrometry* (Marcel Dekker, 1969), Vol. 1.
24. J. Elhanan and W. D. Cooke, "Factors affecting line intensities in the flame spectrometry of metals in organic solvents," Anal. Chem. **38**, 1062–1063 (1966).

25. R. Avni and C. T. J. Alkemade, "The role of some organic solvents in flame photometry," Microchimica Acta **48**, 460–471 (1960).
26. G. V. Deverall, K. W. Meissner, and G. J. Zissis, "Hyperfine structures of the resonance lines of indium," Phys. Rev. **91**, 297–299 (1953).
27. J. Casas, J. S. C. Fernádez, and J. Sordo, *Lead: Chemistry, Analytical Aspects, Environment Impact & Health Effects* (Elsevier Science, 2006).
28. L. Bütfering, G. Schmelzeisen-Redeker, and F. W. Röllgen, "Studies with a dual-beam thermospray interface in high-performance liquid chromatography mass spectrometry," J. Chromatogr. **394**, 109–116 (1987).
29. G. Schmelzeisen-Redeker, L. Bütfering, and F. W. Röllgen, "Desolvation of ions and molecules in thermospray mass spectrometry," Int. J. Mass Spectrom. Ion Processes **90**, 139–150 (1989).
30. V. A. Fassel, J. O. Rasmuson, R. N. Kniseley, and T. G. Cowley, "Relative free-atom populations in nitrous oxide-acetylene flames used in analytical spectroscopy," Spectrochim. Acta Part B **25**, 559–575 (1970).
31. P. Rajan and A. B. Pandit, "Correlations to predict droplet size in ultrasonic nebulization," Ultrasonics **39**, 235–255 (2001).
32. R. J. Lang, "Ultrasonic atomization of liquids," J. Acoust. Soc. Am. **34**, 6–8 (1962).
33. D. Sindayihebura, M. Dobre, and L. Bolle, "Experimental study of thin liquid film ultrasonic atomization," in *4th World Conference on Experimental Heat Transfer, Fluid Mechanics and Thermodynamics* (Edizioni ETS, 1997), pp. 1249–1256.
34. W. Wang, A. Purwanto, I. W. Lenggoro, K. Okuyama, H. Chang, and H. D. Jang, "Investigation on the correlations between droplet and particle size distribution in ultrasonic spray pyrolysis," Ind. Eng. Chem. Res. **47**, 1650–1659 (2008).
35. A. Balasubrahmanyam, M. N. Patil, P. R. Gogate, and A. B. Pandit, "Ultrasonic atomization: effect of liquid phase properties," Ultrasonics **44**, 146–158 (2006).
36. R. K. Winge, V. A. Fassel, and R. N. Kniseley, "Direct nebulization of metal samples for flame atomic-emisson and absorption spectroscopy," Appl. Spectrosc. **25**, 636–642 (1971).
37. R. M. Frinstrom and A. A. Westenberg, *Flame Structure* (McGraw-Hill, 1965).
38. C. G. Fotache, T. G. Kreutz, D. L. Zhu, and C. K. Law, "An experimental study of ignition in nonpremixed counterflowing hydrogen versus heated air," Combust. Sci. Technol. **109**, 373–393 (1995).
39. J. B. Willis, "Atomization problems in atomic absorption spectroscopy–i. A study of the operation of a typical nebulizer, spray chamber and burner system," Spectrochim. Acta Part A **23**, 811–830 (1967).
40. L. R. Snyder and J. J. Kirkland, *Introduction to Modern Liquid Chromatography*, 2nd. ed. (Wiley, 1979).
41. K. Fujiwara, H. Haraguchi, and K. Fuwa, "Profiles of the distribution of atoms in the nitrous oxide-acetylene flame," Bull. Chem. Soc. Jpn. **48**, 857–862 (1975).